

Supplementary Information

Controlling CO₂ flux in a CO₂-permeable membrane with a H₂O driving force

Jacqueline A. Penn,^a Wenting Hu,^a Ian S. Metcalfe^a and Greg A. Mutch*^a

^a *Materials, Concepts & Reaction Engineering (MatCoRE) Group, School of Engineering, Newcastle University, Newcastle upon Tyne, NE1 7RU, UK. Email: greg.mutch@newcastle.ac.uk*

Supplementary Figure 1: Membrane reactor and flow system	1
Supplementary Figure 2: Membrane reactor residence time distribution	2
Supplementary Figure 3: Calibration of H₂O concentration in gas streams	4
Supplementary Table 1: Accuracy of titration against known mixtures of carbonates and hydroxides	5
Supplementary Table 2: The effect of cooling procedures on recovered salt composition	6
Supplementary Figure 4: SEM images of the membrane support before and after operation	7
Supplementary Table 3: EDX analysis of the membrane support before and after operation	8
Supplementary Figure 5: Raman spectra of the membrane support before and after operation	11
Supplementary Figure 6: Example experimental traces from time series	12
Supplementary Table 4: Permeation experiments flux and titration data reported in Fig. 4a	13
Supplementary Figure 7: Example experimental traces from H₂O concentration series	14
Supplementary Table 5: Permeation experiment repeats reported in Fig. 4b	15
Supplementary Figure 8: CO₂ flux at 500, 600, and 700 °C with 10 and 50% CO₂ in N₂ feed gases	16
Supplementary Table 6: Molten salt composition with 10 and 50% CO₂ in N₂ feed gases	17
References	18

Supplementary Figure 1: Membrane reactor and flow system

The supported molten-salt membrane was housed in a custom-made membrane reactor (Fig. S1a), with gases supplied by a bespoke flow system (Fig. S1b,c).

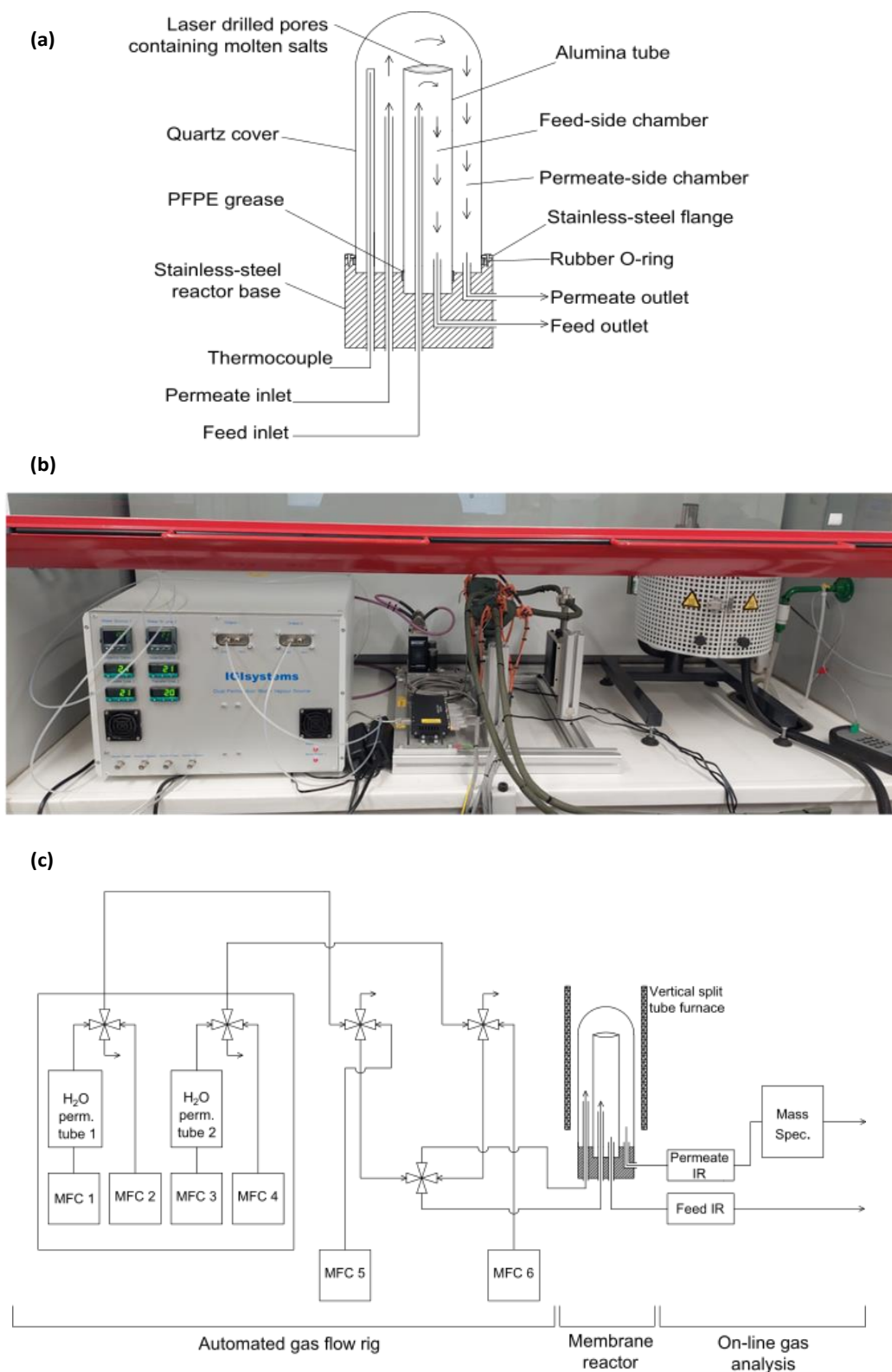


Fig. S1 Membrane reactor and flow system. (a) Schematic of custom-made membrane reactor. (b) Photograph of flow system. (c) Schematic of flow system. Note that the reactor (a) is designed such that the base sits outside the hot zone of the furnace in (b), to permit the use of vacuum grease and an O-ring for sealing.

Supplementary Figure 2: Membrane reactor residence time distribution

The residence times of the feed- and permeate-side chambers were determined by monitoring the outlets of the reactor with a mass spectrometer following an inert gas step-change.¹

The cumulative distribution function $F(t)$ of the step input was plotted (**Fig. S2**) using **Equation S1**, where C_{outlet} is the concentration of the outlet gas, C_{inlet} is the inlet concentration, and t is time.

$$F(t) = \left[\frac{C_{outlet}(t)}{C_{inlet}} \right]_{step} \quad \text{Equation S1}$$

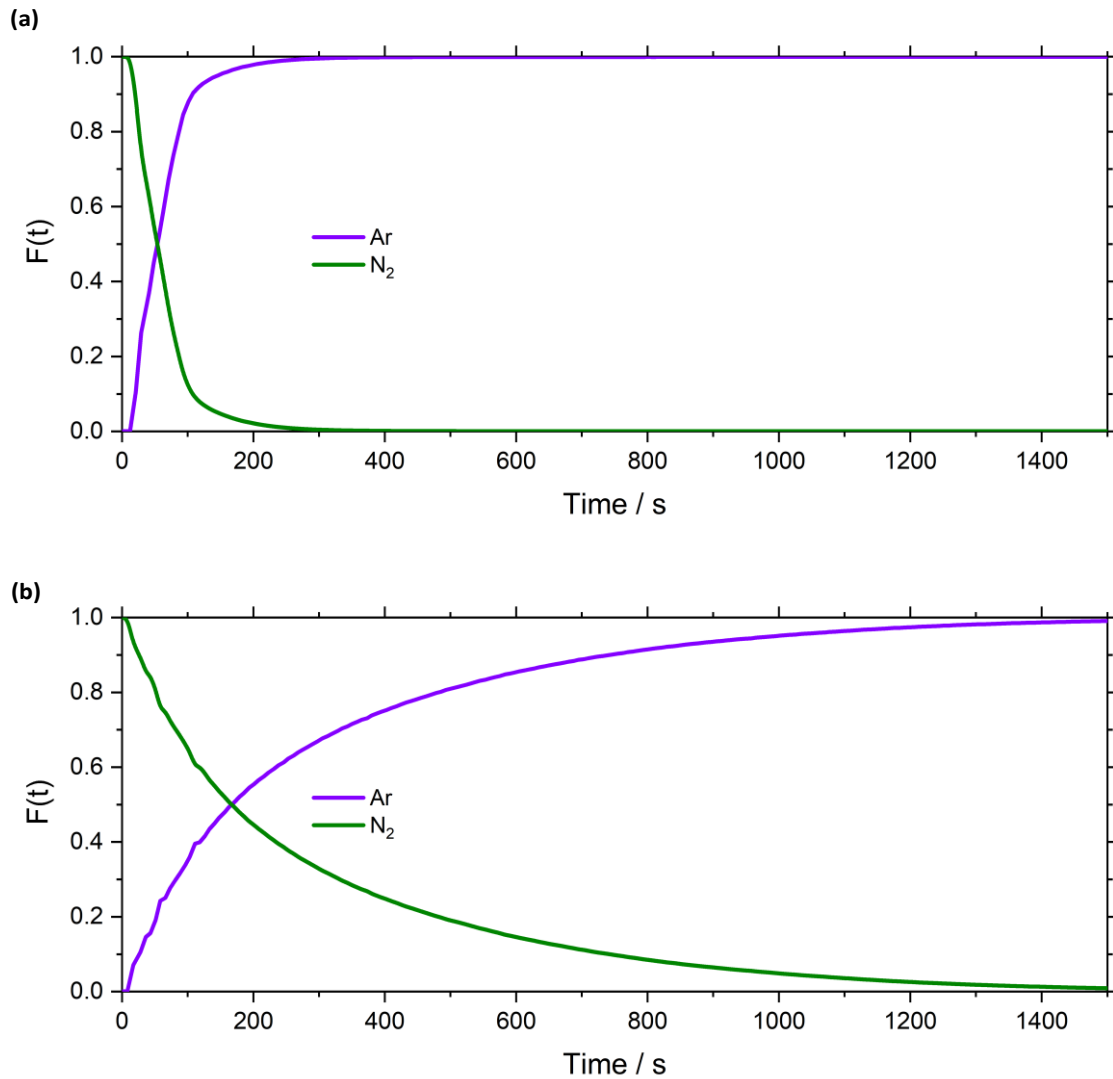


Fig. S2 Membrane reactor residence time distribution. Cumulative distribution function $F(t)$ for the feed- (a) and permeate-side (b) chambers, respectively.

The cumulative distribution function $F(t)$ was differentiated to plot the residence time distribution function $E(t)$ using **Equation S2**,

$$E(t) = \frac{d}{dt} \left[\frac{C_{outlet}(t)}{C_{inlet}} \right]_{step} \quad \text{Equation S2}$$

The residence time distribution $E(t)$ was used to calculate the mean residence time t_m using **Equation S3**,

$$t_m = \int_0^{\infty} tE(t)dt \quad \text{Equation S3}$$

The mean residence time of the feed- and permeate-side chambers were 61 and 250 s, respectively.

The volume (V) of each chamber of the reactor was calculated from the mean residence time (t_m) and the volumetric flowrate (v) using **Equation S4**,

$$V = vt_m \quad \text{Equation S4}$$

The volumes of the feed- and permeate-side chambers calculated from the mean residence time were 29 and 114 cm³, respectively. This compared to estimated volumes (based on the dimensions of the chambers) of 39 and 170 cm³, respectively. As the calculated volumes were ~25–30% lower than the estimated volumes, it is possible that there were stagnant zones in the membrane reactor. However, due to the design of the membrane reactor (particularly the proximity of the gas inlets to the membrane surfaces), we expect the stagnant zones were around the gas inlet tubes and they are therefore not expected to significantly impact the composition that the membrane surface was exposed to.

Supplementary Figure 3: Calibration of H₂O concentration in gas streams

The flow system permitted the independent humidification of the gases supplied to the feed- and permeate-side chambers (i.e., the feed and sweep gas respectively), due to the presence of two in-line, water-filled permeation tubes. These consist of two water-filled reservoirs, separated from the gas streams by two water-permeable membranes, contained within two furnaces. The quantity of water transferred across the water-permeable membranes, and therefore the resulting H₂O concentration in the gas streams, was controlled by varying the temperature of the furnaces.

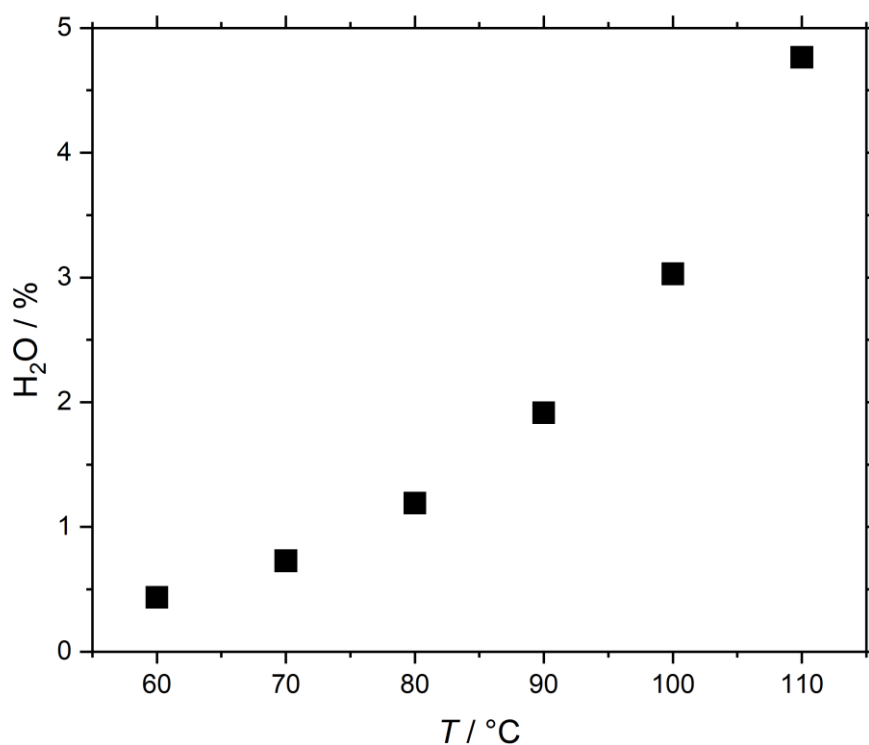


Fig. S3 Calibration of H₂O concentration in gas streams. H₂O concentration in a 50 ml min⁻¹ flow of Ar as a function of water permeation-tube furnace temperature.

Supplementary Table 1: Accuracy of titration against known mixtures of carbonates and hydroxides

To test the reliability of the titration, physical mixtures of carbonates and hydroxides of known composition (between 100 mol% carbonate and 100 mol% hydroxide) were prepared by weighing out and mixing samples of the eutectic carbonate mixture (43.5 mol% Li_2CO_3 , 31.5 mol% Na_2CO_3 , and 25 mol% K_2CO_3) and hydroxide mixture (43.5 mol% LiOH , 31.5 mol% NaOH , and 25 mol% KOH). The physical mixtures were then dissolved in deionised water before analysis by titration to replicate the recovery of salts following permeation experiments. The titration was found to be highly reliable, with the largest difference between actual and measured composition being <4% (Table S1).

Table S1 Titration testing with known mixtures. Known refers to prepared mixtures, measured to titration results, and difference is the difference between these.

Target $\text{OH}^-:\text{CO}_3^{2-}$ Ratio	Known $\text{OH}^- / \%$	Known $\text{CO}_3^{2-} / \%$	Measured $\text{OH}^- / \%$	Measured $\text{CO}_3^{2-} / \%$	Difference $\text{OH}^- / \%$	Difference $\text{CO}_3^{2-} / \%$
100:0	100	0	100.11	-0.11	0.11	-0.11
90:10	90.16	9.84	89.33	10.67	0.83	-0.83
80:20	80.75	19.25	82.35	17.65	-1.60	1.60
75:25	74.77	25.23	77.06	22.94	-2.29	2.29
50:50	50.96	49.04	54.67	45.33	-3.71	3.71
25:75	25.78	74.22	26.14	73.86	-0.36	0.36
0:100	0	100	1.27	98.73	1.27	-1.27

Supplementary Table 2: The effect of cooling procedures on recovered salt composition

The composition of salts recovered following different cooling procedures (from membrane operating conditions to salt recovery at room temperature) was performed to test whether the cooling rate and atmosphere had a significant effect on salt composition. Four molten hydroxide membranes were heated to 600 °C and exposed to 50% CO₂ in N₂ for 1 h. Subsequently, they were cooled at 2 or 5 °C min⁻¹ in either 50% CO₂ in N₂ or Ar. The composition of the recovered salts was found to be similar, suggesting that the cooling procedure did not significantly impact salt composition (**Table S2**).

Table S2 Cooling procedures and recovered salt composition.

Cooling Procedure	Measured OH ⁻ / %	Measured CO ₃ ²⁻ / %
2 °C min ⁻¹ in Ar	40	60
5 °C min ⁻¹ in Ar	42	58
2 °C min ⁻¹ in 50% CO ₂ in N ₂	44	56
5 °C min ⁻¹ in 50% CO ₂ in N ₂	36	64

Supplementary Figure 4: SEM images of the membrane before and after operation

The laser-drilled Al_2O_3 membrane support was characterised using SEM after two cuts with a diamond saw; the first to remove the laser-drilled closed end, and the second to prepare a cross-section. There were no significant changes to the physical properties of the support (e.g., overall geometry, laser-drilled hole size and shape, membrane thickness etc) (Fig. S4). Subtle changes to the textural properties of the surfaces exposed to molten salts (compare Fig. S4d,e,i,j to Fig. S4n,o,s,t) were investigated using EDX (Table S3) and Raman spectroscopy (Fig. S5).

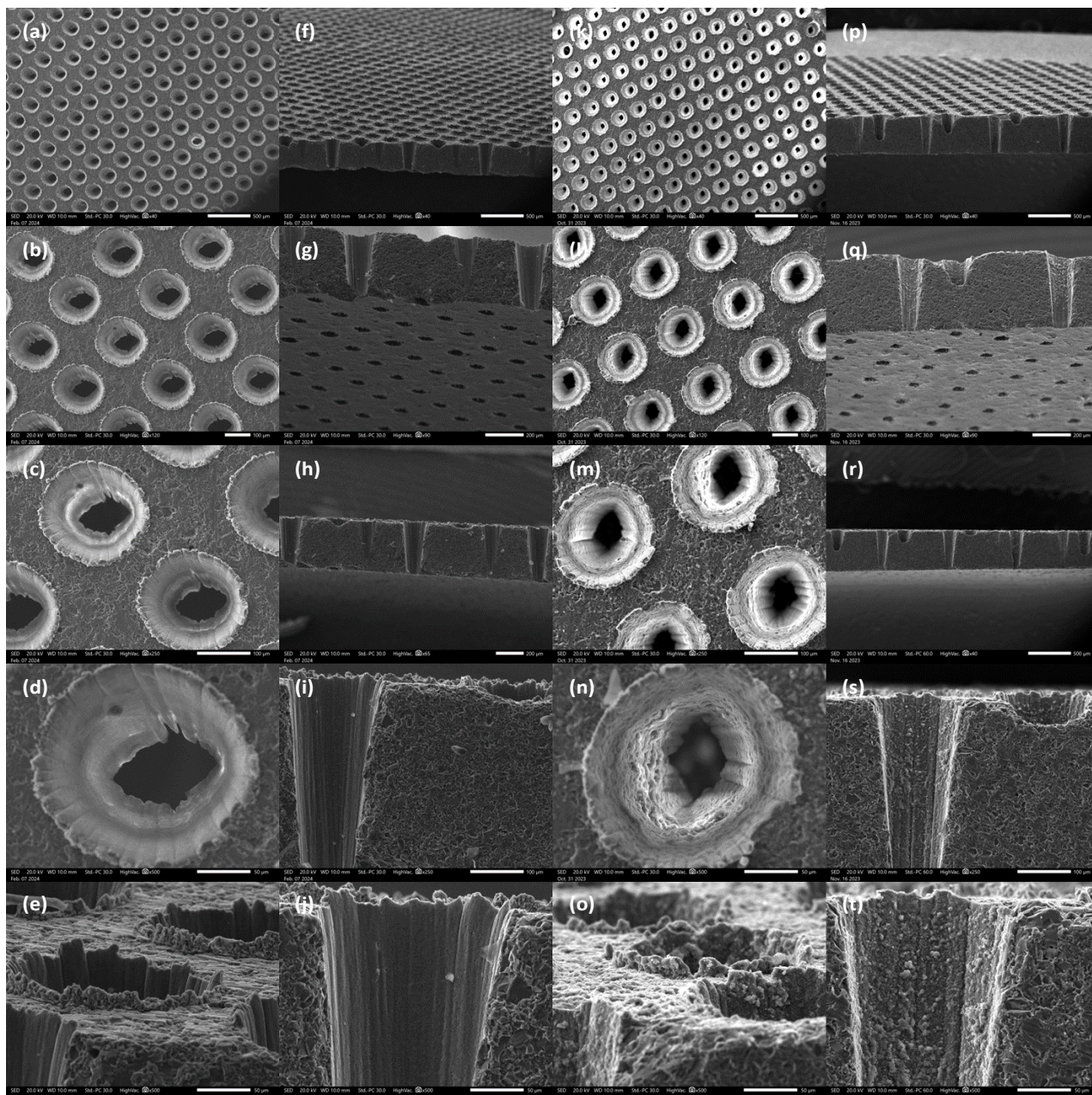
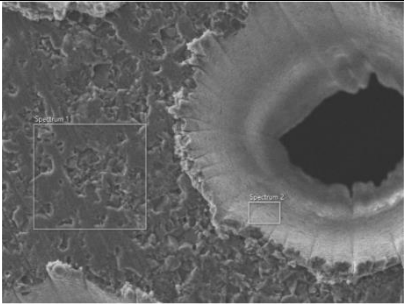
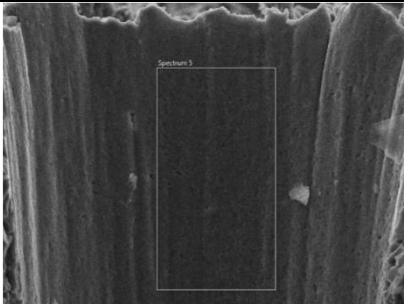
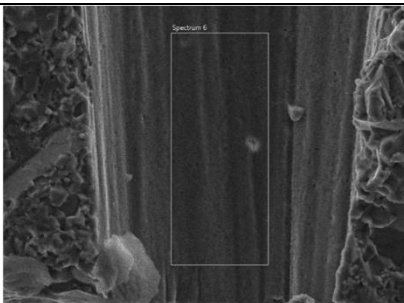
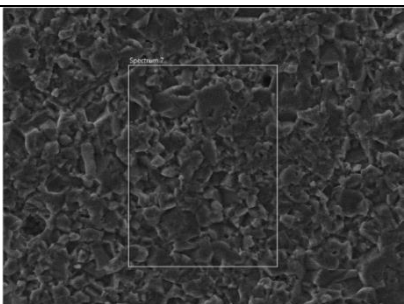


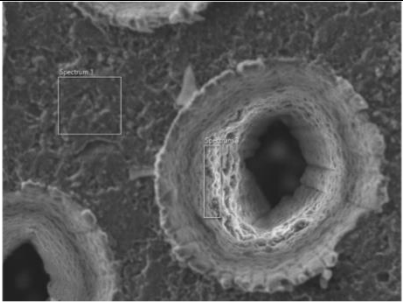
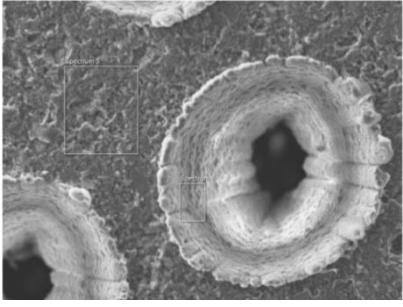
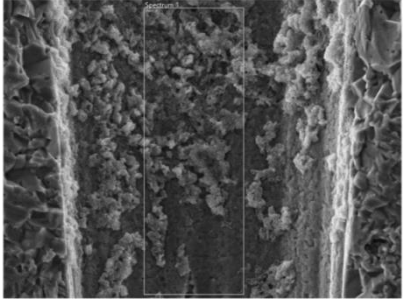
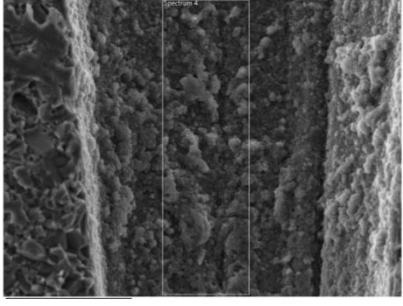
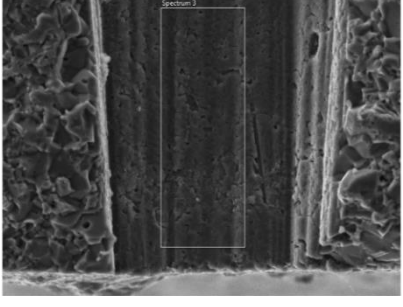
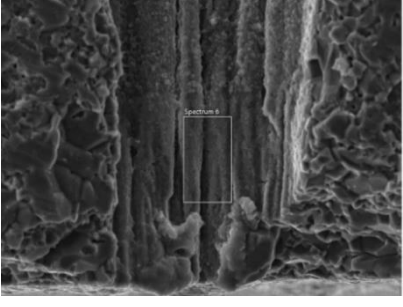
Fig. S4 SEM images of the membrane support. Top-down (a-e) and cross-section (f-j) views of the support before use, and top-down (k-o) and cross-section (p-t) views of the support following ~800 h of operation (several extended permeation experiments, including ~500 h at 400 – 700 °C whilst measuring gas permeation, and ~300 h of heating/cooling).

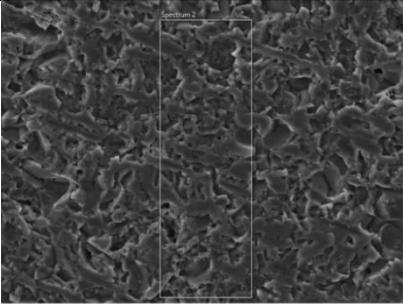
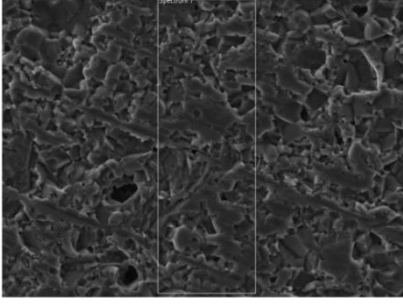
Supplementary Table 3: EDX analysis of the membrane support before and after operation

Elemental composition of the membrane support before use, and following ~800 h of operation was determined using EDX (**Table S3**). Al and O were detected in all samples, as was C (due to carbon coating), with small amounts of Si and F also present in some samples (likely due to impurities). The Al:O ratio was analysed; Al_2O_3 has an Al:O ratio of 1:1.67, whereas LiAlO_2 Li_5AlO_4 are 1:2 and 1:4, respectively. The Al:O ratio corresponded well with Al_2O_3 in all analysed locations of the membrane support before use, whereas following operation, there was a consistent decrease in the Al:O ratio in all locations exposed to molten hydroxides, suggesting the formation of LiAlO_2 and/or Li_5AlO_4 , consistent with Raman analysis (**Fig. S5**).

Table S3 EDX analysis of the membrane support.

Sample	Location	Al / %	O / %	Al:O
Before use		27.1	45.1	1:1.66
		24.1	39.3	1:1.63
		23.5	38.9	1:1.66
		22.7	36.6	1:1.61

Following ~800 h operation		24.6	48.3	1:1.96
		24.2	48.9	1:2.05
		16.1	54.0	1:3.35
		13.7	55.8	1:4.07
		19.7	50.5	1:2.56
		17.3	46.5	1:2.68

		20.8	46.2	1:2.22
		20.6	46.6	1:2.26

Supplementary Figure 5: Raman spectra of the membrane support before and after operation

Raman spectra were collected from the laser-drilled hole walls of the membrane support before use and following ~ 800 h of operation (collected from regions like those shown in **Fig. S4j** and **Fig. S4t**, respectively) (**Fig. S5**). Peaks present in both spectra at ~ 380 , 420 , 430 , 650 , and 750 cm^{-1} are characteristic of Al_2O_3 ,² whereas the peaks at ~ 120 , 260 , 360 , 500 , and 600 cm^{-1} (marked with an *) can be assigned to the $\text{B}_2^{(1)}$ LiO_4 - AlO_4 , $\text{B}_1^{(1)}$ Li-O-Al stretching, $\text{E}^{(2)}$ Li-O bending, $\text{E}^{(3)}$ Al-O bending, and $\text{E}^{(4)}$ Al-O bending modes in LiAlO_2 .³ We note that peaks assigned to LiAlO_2 were not observed on the surfaces revealed during preparation of the cross-section of the support following ~ 800 h of operation.

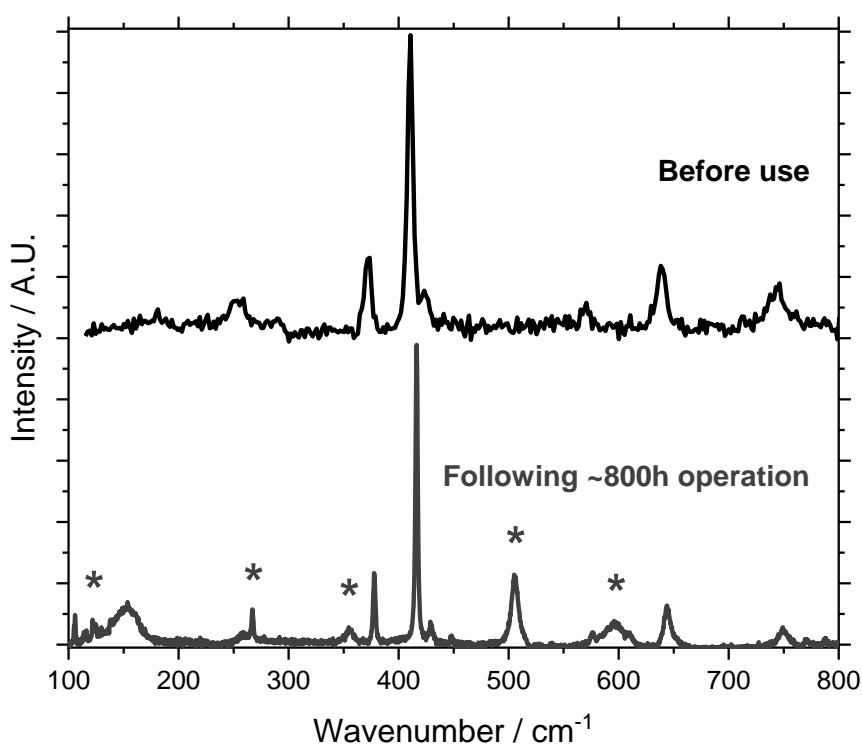


Fig. S5 Raman spectra of the membrane support. The *s highlight features assigned to LiAlO_2 in the support following operation for ~ 800 h, whereas all other features in both spectra are assigned to Al_2O_3 .

Supplementary Figure 6: Example experimental traces from time series

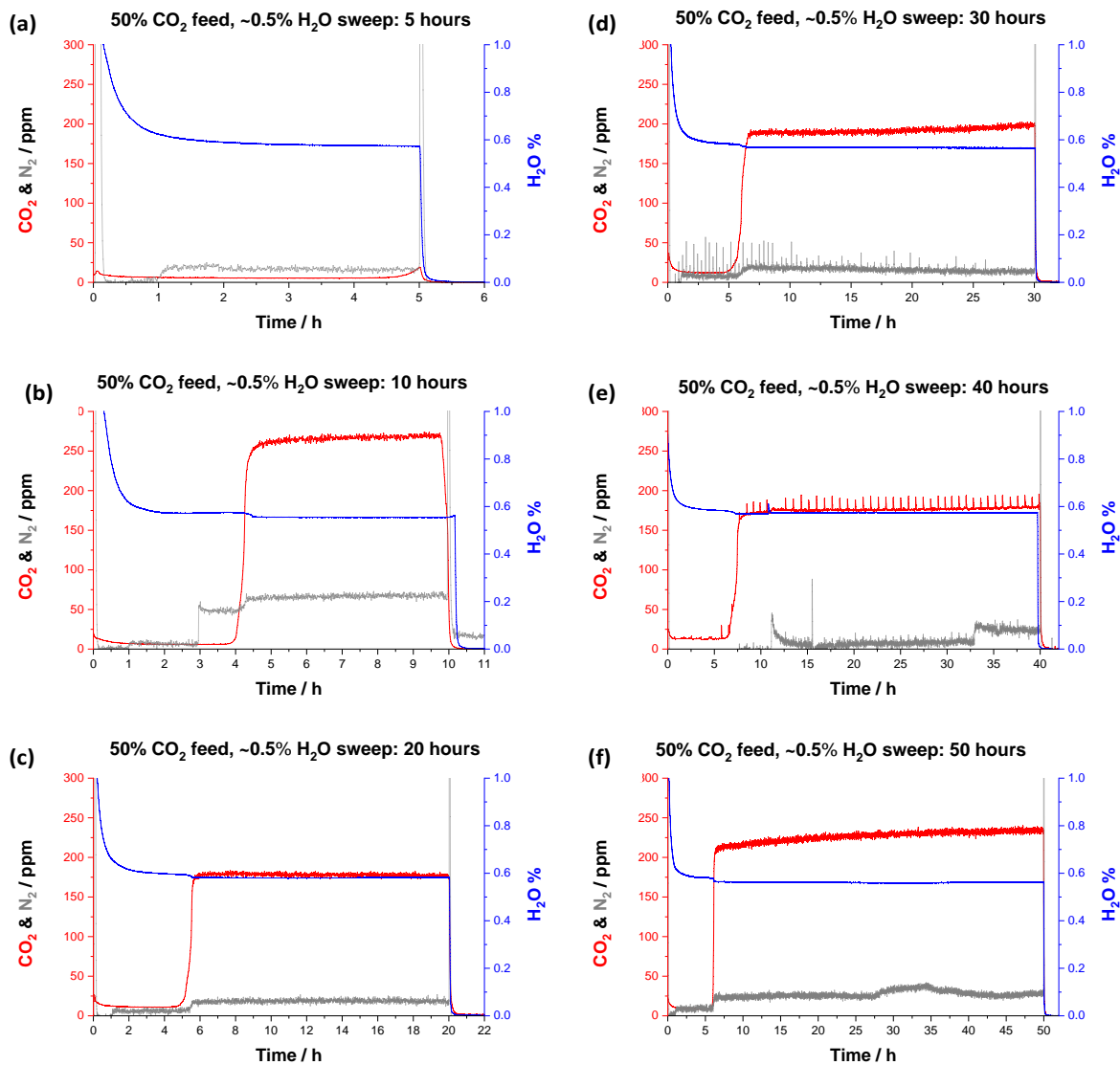


Fig. S6 CO₂, N₂, and H₂O concentration as a function of time on the permeate-side. In (a-f) the feed gas was 50% CO₂ in N₂, the sweep gas was ~0.5% H₂O, and the temperature was 600 °C. Data used in Fig. 4a.

Supplementary Table 4: Permeation experiments flux and titration data reported in Fig. 4a

The CO₂ flux (points) and titration data (bars) reported in **Fig. 4a** are provided in **Table S4**. The CO₂ flux corresponds with the data shown in **Fig. S6**.

Table S4 Permeation experiments and titration data shown in Fig 4a. The * denotes that the membrane was heated to 600 °C with ~1% H₂O in Ar supplied to both the feed- and permeate-side chamber inlets but cooled in dry Ar without being exposed to the 50% CO₂ in N₂ feed gas. In all other experiments, following the heating, the feed-side chamber inlet was switched to 50% CO₂ in N₂ and the permeate-side chamber inlet was switched to ~0.5% H₂O in Ar.

Length of experiment (time membrane exposed to CO ₂ feed gas)	CO ₂ Flux / 10 ⁻⁴ mol s ⁻¹ m ⁻²	Titration	
		Measured OH ⁻ / %	Measured CO ₃ ²⁻ / %
<i>t</i> / h			
0*	-	91.2	8.8
5	0.20	41.1	58.6
10	2.86	29.7	70.3
20	1.85	47.2	52.8
30	2.11	41.7	58.3
40	2.02	41.1	58.9
50	1.85	41.9	58.1

Supplementary Figure 7: Example experimental traces from H₂O concentration series

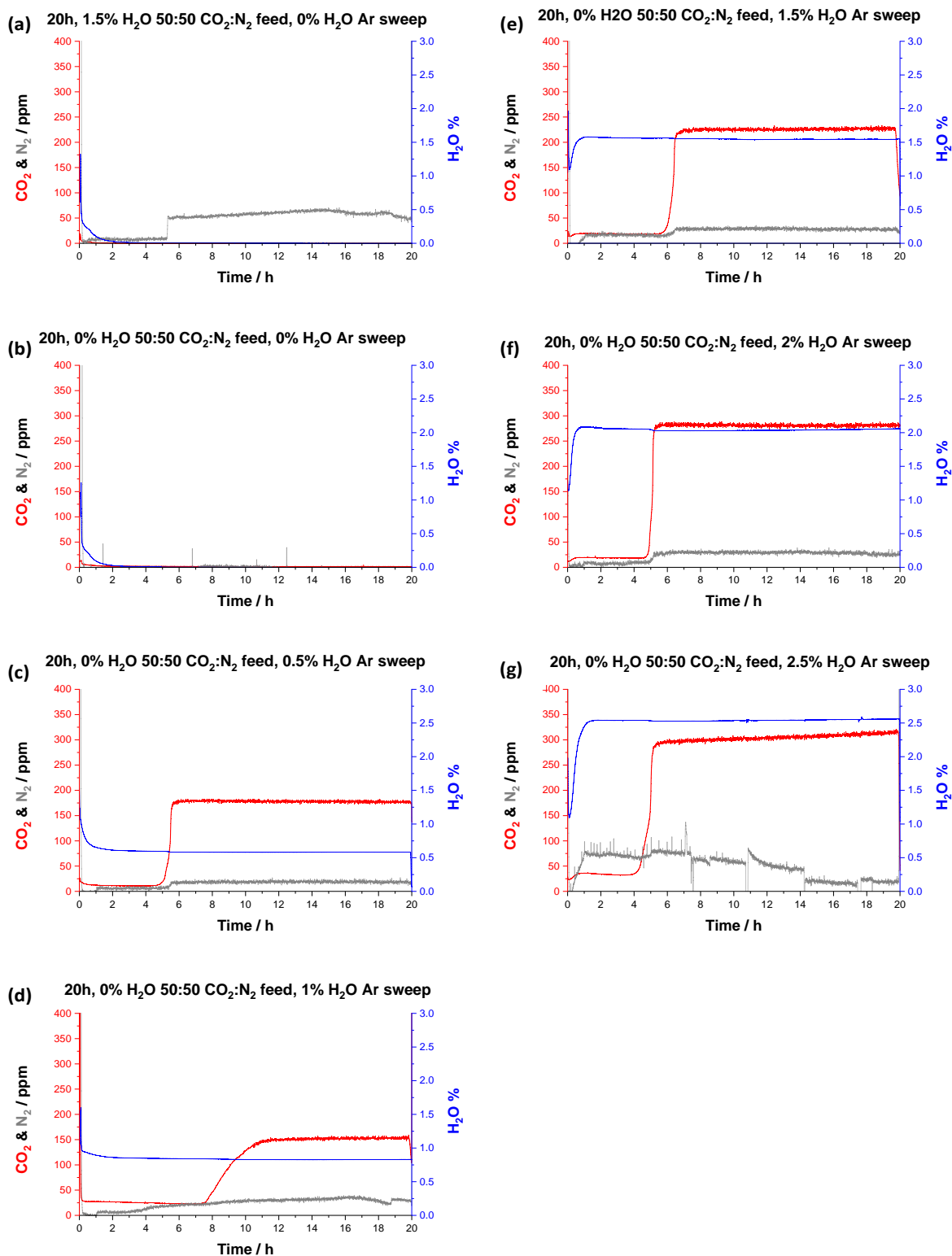


Fig. S7 CO₂, N₂, and H₂O concentration as a function of time on the permeate-side. In (a) the feed gas was 50% CO₂ in N₂ with ~1.5% H₂O, and in (b-g) the feed gas was 50% CO₂ in N₂ whilst the sweep gas H₂O concentration was varied. The temperature was 600 °C throughout. Data used in Fig. 4b.

Supplementary Table 5: Permeation experiment repeats reported in Fig. 4b

CO₂ flux measurements were repeated up to four times, to assess experimental uncertainty. In **Fig. 4b**, CO₂ flux (points) are the mean flux and error bars on the CO₂ flux are the standard deviation reported in **Table S5**. Also, the titration data reported in **Fig. 4b** is that provided in **Table S5**. Repeat 1 in **Table S5** corresponds with the data in **Fig. S7** as does the titration data.

Table S5 Permeation experiment repeats. The * denotes that H₂O was added to the feed gas (in all other cases H₂O was added to the sweep gas).

H ₂ O / %	CO ₂ Flux / 10 ⁻⁴ mol s ⁻¹ m ⁻²						Titration	
	Repeat 1	Repeat 2	Repeat 3	Repeat 4	Mean	Standard Deviation	Measured OH ⁻ / %	Measured CO ₃ ²⁻ / %
1.5*	0.000026	0.50	-	-	0.25	0.35	74.1	25.9
0	0.015	0.21	0.23	0.26	0.18	0.11	70.4	29.6
0.5	1.83	2.09	2.00	2.47	2.10	0.27	47.2	52.8
1.0	1.64	2.73	2.79	-	2.39	0.65	42.7	57.3
1.5	2.40	3.27	-	-	2.84	0.61	46.5	53.5
2.0	2.99	3.06	-	-	3.02	0.05	49.4	50.6
2.5	3.40	3.47	-	-	3.43	0.05	42.0	58.0

Supplementary Figure 8: CO₂ flux at 500, 600, and 700 °C with 10 and 50% CO₂ in N₂ feed gases

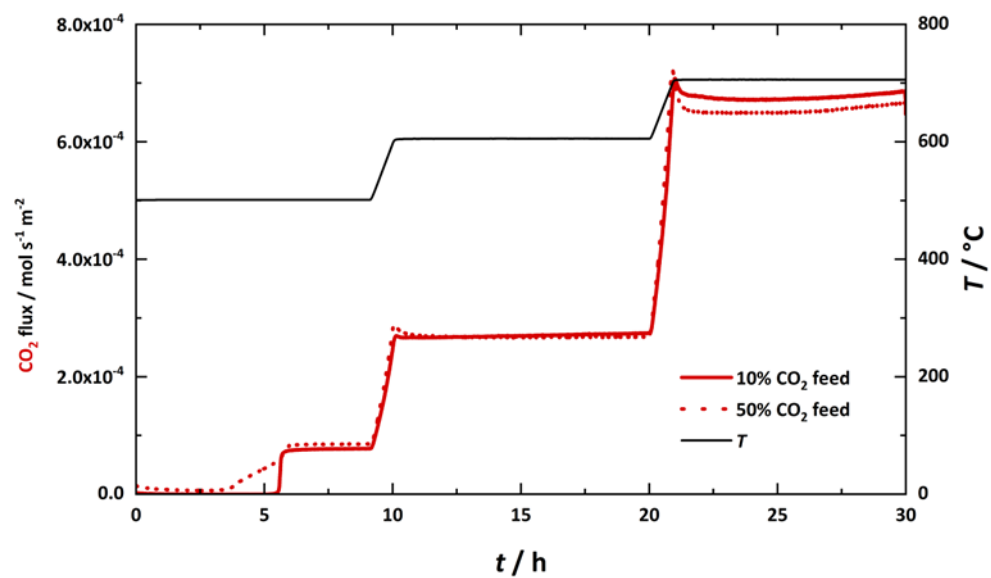


Fig. S8 CO₂ flux as a function of feed gas and temperature. CO₂ flux (measured at the permeate-side outlet). Feed-side chamber inlet: 10 or 50% CO₂ in N₂. Permeate-side chamber inlet: ~1% H₂O in Ar. $T = 500, 600, \text{ and } 700 \text{ }^\circ\text{C}$.

Supplementary Table 6: Molten salt composition with 10 and 50% CO₂ in N₂ feed gases

Salts were recovered from two separate permeation experiments with 10 and 50% CO₂ in N₂ feed gases, both having a ~0.5% H₂O in Ar sweep gas, and having been held for 10 h at 500, 600, and 700 °C. The carbonate:hydroxide ratios measured by titration were comparable within the uncertainty of the titration.

Table S6: Feed gas and recovered salt composition. Values are provided as the mean of triplicate titrations with standard deviation.

Feed Gas	Measured OH⁻ / %	Measured CO₃²⁻ / %
10% CO₂ in N₂	23 ± 2	77 ± 3
50% CO₂ in N₂	14 ± 13	86 ± 15

References

- 1 H. S. Fogler, in *Elements of Chemical Reaction Engineering, 4th Edition*, Pearson, 2006, pp. 878–942.
- 2 R. Krishnan, R. Kesavamoorthy, S. Dash, A. K. Tyagi and B. Raj, *Scr. Mater.*, 2003, **48**, 1099–1104.
- 3 Q. Hu, L. Lei, X. Jiang, Z. C. Feng, M. Tang and D. He, *Solid State Sci.*, 2014, **37**, 103–107.